

SEMICONDUCTOR SURFACE AND INTERFACE  
DYNAMICS FROM TIGHT-BINDING MOLECULAR  
DYNAMICS SIMULATIONS

G. K. Schenter  
J. P. LaFemina

November 1991

Presented at the  
38th Annual AVS Symposium and  
Topical Conference  
November 11-15, 1991  
Seattle, Washington

Work supported by  
the U.S. Department of Energy  
under Contract DE-AC06-76RLO 1830

Pacific Northwest Laboratory  
Richland, Washington 99352

**DISCLAIMER**

This report was prepared as an account of work sponsored by an agency of the United States Government. Neither the United States Government nor any agency thereof, nor any of their employees, makes any warranty, express or implied, or assumes any legal liability or responsibility for the accuracy, completeness, or usefulness of any information, apparatus, product, or process disclosed, or represents that its use would not infringe privately owned rights. Reference herein to any specific commercial product, process, or service by trade name, trademark, manufacturer, or otherwise does not necessarily constitute or imply its endorsement, recommendation, or favoring by the United States Government or any agency thereof. The views and opinions of authors expressed herein do not necessarily state or reflect those of the United States Government or any agency thereof.

MASTER



Abstract # : 328  
Program # : SS-TuP48  
Put on JVST manuscript

Semiconductor Surface and Interface Dynamics  
from Tight-Binding Molecular Dynamics Simulations

Gregory K. Schenter and John P. LaFemina

*Molecular Science Research Center  
Pacific Northwest Laboratory\*  
P.O. Box 999  
Richland, Washington 99352*

-----  
\*Operated for the US Department of Energy by Battelle Memorial Institute under contract DE-AC06-76RL01830

## Abstract

Tight-binding molecular dynamics simulations have been performed to compute the bulk, (110) surface, and (110)-p(1x1)-Sb(1ML) interfacial atomic vibrational spectra for GaAs and InP. The same tight-binding total energy model which successfully described the static surface and interfacial atomic and electronic structure for these systems is utilized in the molecular dynamics simulations. The results for the bulk vibrational energies are in semi-quantitative agreement with experimental results, displaying approximately the same level of variance as other model computations. Moreover, these simulations are used to examine the effects of anharmonicity in the system by investigating the temperature dependence of the vibrational spectra. The (110) surface vibrational energies are in quantitative agreement with the scattering data, and a comparison of the results for GaAs(110) and InP(110) supports the existence of a surface vibrational mode which is characteristic of the relaxed (110) surface, and whose energy is similar for each zincblende (110) surface. Lastly, the computed vibrational energies for the III-V(110)-p(1x1)-Sb(1ML) interface are in semi-quantitative agreement with Raman scattering data and illustrate the effects of the overlayer binding on the surface vibrational spectrum.

## I. Introduction

Quantum-mechanical molecular dynamics (QMMD) simulations, based upon local-density functional<sup>1,2</sup> and tight-binding<sup>3,4,5</sup> (TB) Hamiltonians, have recently been used to examine the structural and harmonic, as well as anharmonic, vibrational properties of Column IV microclusters<sup>2,3,5</sup> and bulk material<sup>4</sup>. In addition, molecular dynamics (MD) based simulated annealing computations have been carried out on both clean<sup>6,7</sup> and adsorbed<sup>7</sup> semiconductor surfaces to determine the nature of surface and interface geometries. One advantage to the use of MD simulations over conventional quantum-mechanical computations of total-energy derivative properties is the ability of MD simulations to investigate anharmonicity<sup>4</sup> obtained from a direct dynamical sampling. The applicability of these methods to the study of the vibrational properties of surfaces has been stated in the literature<sup>2,3,4</sup> although we are unaware of any published work in this area.

Epitaxial monolayers of Sb on III-V(110) surfaces are of interest in semiconductor surface science because they form ordered, chemically saturated overlayers which are the precursors to metal-semiconductor contacts. Their atomic geometries are known quantitatively from analyses of low-energy electron diffraction intensities<sup>8,9</sup> and x-ray standing-wave studies<sup>10</sup> for GaAs(110)-p(1x1)-Sb(1ML)<sup>8-10</sup> and InP(110)-p(1x1)-Sb(1ML)<sup>10</sup>. Moreover, these geometries have been predicted quantitatively for GaAs(110)<sup>11</sup>, InP(110)<sup>11</sup>, GaAs(110)-p(1x1)-Sb(1ML)<sup>12,13</sup>, and InP(110)-p(1x1)-Sb(1ML)<sup>12,13</sup> using tight-binding total energy (TBTE) models which also describe qualitatively the surface electronic states observed by angular-

dependent photoemission. These studies have shown that the (110) surfaces of zincblende-structure materials exhibit a common relaxation, characterized by a nearly-bond-length-conserving rotation of the surface layer of  $29^{\circ} \pm 3^{\circ}$  relative to the ideal surface plane<sup>14</sup>. The adsorption of Sb returns the substrate to a nearly ideal bulk structure through a unique type of chemical bonding between the pi electrons of the top layer Sb zig-zag chain and the  $sp^3$  hybrids of the III-V(110) substrate<sup>12</sup>.

The exploration of the surface atomic dynamics was undertaken initially by Harten and Toennies<sup>15</sup> using inelastic He atom scattering from the GaAs(110) surface. An "optical" surface mode at approximately 10 meV was soon interpreted by Wang and Duke<sup>16</sup> as a characteristic mode of the relaxed (110) surface, corresponding to nearly-bond-length-conserving rotations, about the equilibrium tilt angle, of the top layer relative to the substrate. Doak and Nguyen<sup>17</sup> confirmed and extended the experimental results of Harten and Toennies<sup>15</sup>, with emphasis on the extension to surface phonons along the  $\bar{\Gamma}$ - $\bar{X}'$  line of the surface Brillouin zone. Subsequently, bond-charge slab model calculations of the atomic dynamics of GaAs(110) and further measurements along the  $\bar{\Gamma}$ - $\bar{X}'$  and  $\bar{\Gamma}$ - $\bar{M}$  lines were reported in an attempt to synthesize the existing data<sup>15,17</sup>, the rotational surface mode concepts<sup>16</sup>, and the authors' new data into a single, coherent interpretation of the surface dynamics of GaAs(110)<sup>18</sup>. These calculations suggested that the concept of rigid bond-length-conserving rotations had limited utility in describing the actual surface normal modes of GaAs(110), despite the fact that the energetics predicted by Wang and Duke were correct.

The dynamics of the InP(110)-p(1x1)-Sb interface has been recently examined by Hünemann *et al.*<sup>19</sup> via Raman scattering spectroscopy, and localized surface and interface phonons were identified. In a recent study based on a harmonic dynamical matrix treatment of the surface atomic vibrations, Godin *et al.*<sup>20</sup> explored the surface and interfacial atomic dynamics for GaAs(110) and GaAs(110)-p(1x1)-Sb(1ML) utilizing the same TBTE models used herein, and which were developed previously in static studies of these systems<sup>11-13</sup>. Using a "restricted dynamical model", in which only the surface layer atoms were allowed to move, Godin *et al.*<sup>20</sup> computed the dynamical force fields and surface atomic vibrational spectra, and predicted relationships between the microscopic force constants, the surface vibrational spectrum and normal modes, and the surface atomic and electronic structure. For the GaAs(110) surface, the computed optical mode energies were in quantitative agreement with the He-scattering results<sup>15,17,18</sup> and the results of the bond-charge slab computation<sup>18</sup> suggesting that the restricted dynamical model provides an adequate description of the surface atomic vibrations. One difficulty associated with the computations of Ref. 20 is the need to evaluate numerically the derivative of the total energy for a large number of generalized displacements. As the size of the system to be examined grows, this need can become prohibitive. In addition generalized displacements must be constrained to the harmonic regime. Consequently we have explored the use of molecular dynamics simulations to compute the desired spectral densities. In our studies, the spectral properties are obtained from dynamical averages instead of direct diagonalization. This provides a

natural extension of the harmonic dynamical-matrix analysis to the study of anharmonicity in the tight-binding total energy computation of atomic forces.

Our purpose in this paper is to examine the utility of tight-binding based molecular dynamics simulations by computing the spectral density for the bulk, (110) surfaces, and (110)-p(1×1)-Sb(1ML) interfaces of GaAs and InP. The important aspect of our approach is that we utilize the same tight-binding total-energy (TBTE) model to compute the Hellman-Feynman forces that was used successfully to describe the atomic and electronic structure of these systems<sup>11-13,21,22</sup>. *No reoptimization of the model parameters were made in the determination of vibrational properties.*

We proceed by describing the TBTE molecular dynamics (MD) model in Section II. The results of the computations are presented and discussed in Section III. We conclude with a synopsis.

## II. Tight-Binding Molecular Dynamics Model

The equilibrium geometries and forces are computed using the  $sp^3s^*$  tight-binding total energy (TBTE) model developed by Vogl *et al.*<sup>21</sup>, Chadi<sup>22</sup>, and Mailhiot *et al.*<sup>11</sup>. In this model the total energy is separated into an electronic "band structure" component and an elastic component of near-neighbor bonds:

$$E_{\text{TOT}} = E_{\text{bs}} + U = \sum_{\mathbf{k}, n} E_n(\mathbf{k}) + \sum_{i,j} \left[ U_1 \epsilon_{ij} + U_2 \epsilon_{ij}^2 \right], \quad (1)$$

where  $\epsilon_{ij}$  is the fractional displacement from the equilibrium bond distance and  $U_1$  and  $U_2$  are determined from bulk structure and moduli. The single particle eigenvalues,  $E_n(\mathbf{k})$  are taken from an orthogonal nearest neighbor, Slater-Koster<sup>23</sup> Hamiltonian. The  $\mathbf{k}$  space integration appearing in (1) is accomplished via a quadrature scheme developed by Chadi and Cohen<sup>24</sup> which approximates the integral as a sum of "special  $\mathbf{k}$  points". All required model parameters are taken directly from previous studies<sup>12,13</sup>. It should be noted that a similar model has been developed by Wang, Chan and Ho<sup>4</sup> using a different form of the pair potential,  $U$ , which represents the ion-ion interactions and the correction for the double counting of the electron-electron interaction. No long -range coulomb forces are contained in the TBTE model. This is not an important limitation of the model for the  $\mathbf{k}$ -vectors sampled by He-scattering and Raman scattering experiments, nor is it critical to the investigation of trends in phonon dispersion across homologous materials<sup>20</sup>.

In the computation of the Hellman-Feynman forces to drive the molecular dynamics a single "special point" was used<sup>24</sup>. The dynamical matrix studies based on the same energy expression have indicated that this approximation results in a 10% uncertainty in the phonon energies<sup>20</sup>. We find a similar insensitivity of the number of special points to the resulting spectral density as obtained from dynamical analysis.

In the MD simulation, the Hellman-Feynman forces are calculated with periodic boundary conditions across a non-primitive unit cell. Consequently, the frequency distribution obtained from an analysis of velocity autocorrelation of the



motion corresponds to zero wave vector ( $q'=0$ ) motion of this non-primitive unit cell. In the harmonic limit (low temperature),  $3N-1$  modes are expected to be observed where  $N$  is the number of atoms in cell. Due to the symmetry of the crystal, many of these are degenerate. Information of the characteristic motion in the primitive unit cell is contained in the analysis of the non-primitive cell, and may be deconvoluted through band folding. In this, the  $q \neq 0$  motions of the primitive unit cell are transformed to the  $q'=0$  motion for the non-primitive unit cell. For the simulations of bulk GaAs reported in this work the cubic 8-atom non-primitive unit cell shown in Figure 1 was used. The use of this non-primitive cell allows the motion corresponding to the  $\Gamma$  and X phonon modes to be observed in the calculated spectral density. Additional peaks appear which correspond to linear combinations of these modes and are similar to but not identical to the L motion of the primitive cell. For the (110) surface, a 15 atomic-layer slab is used to model the semi-infinite surface (Figure 2). By allowing only the atoms in first two atomic layers to move with the remainder of the layers frozen in their equilibrium configuration, the surface atomic vibrational energies are obtained. One consequence of this approximation is that the surface acoustic modes have non-zero energies at  $q=0$ . This is not a serious limitation of the model since we wish to focus on the surface optical modes. Moreover, the use of this restricted dynamical model<sup>19</sup> is justified due to the fact that the optical eigenmodes of the surface phonons are dominated by displacements of the surface atomic layer<sup>20</sup>. In addition, it is at the surface layer where the most significant bonding and electronic structure changes

occur.

In the dynamical simulations the Verlet algorithm<sup>25,26</sup> was used to propagate the positions and velocities of atomic nuclei as a function of time within a constant energy ensemble. Initial velocities were distributed according to a Maxwellian velocity distribution corresponding to the simulation temperature. The timesteps for the simulations as indicated in Table I were chosen so that energy was conserved to within 0.05% of the total energy. Also indicated in Table I are the number of correlation steps and the number of samples for each run, so that the total number of simulation steps is the product of these two numbers. Throughout the course of the dynamical simulation velocity autocorrelation was accumulated as

$$C(\mathbf{q}, t) = \alpha \sum_{i=1}^N \langle \mathbf{v}_i(t) \cdot \mathbf{v}_i(0) \rangle \quad (2)$$

where  $\alpha$  is a normalization constant,  $\mathbf{v}_i(t)$  represents the velocity of the  $i$ th atom at time  $t$ , and the averages were estimated from

$$\langle f(i\Delta t)f(0) \rangle \approx \frac{1}{n-i+1} \sum_{j=0}^{n-1} f((i+j)\Delta t)f(j\Delta t) \quad (3)$$

Here  $n$  is the total correlation length. A Fourier transform of (2) was made to give an estimate of the configuration averaged spectral density at the end of the simulation.

### III. Results

#### A. Bulk Dynamics

The phonon frequency distribution at 300K and 77K for bulk GaAs and at 300K, 77K, and 2K for InP are shown in Figure 3. As described in the previous section, the use of an 8-atom unit cell in MD simulation results in the frequency distribution containing the phonon frequencies at both  $\Gamma$  and X. These results are summarized in Table II along with the results of several other computational studies<sup>27,29</sup> and experimentally determined phonon frequencies for comparison<sup>28</sup>. As is evident from Table II, the TB-MD frequencies, are in semi-quantitative agreement with the experimental results, with maximum variance for the high energy optical modes. This level of variance is not uncommon however, as is apparent from the results of frozen phonon<sup>29</sup> computations also shown in Table II.

As temperature increases the spectral peaks tend to broaden with the largest spread appearing in the optical modes. Since a completely harmonic system exhibits no spread in spectral density, we attribute the observed behavior to anharmonicity. A slight softening of these modes with increasing temperature is also observed. These effects are more pronounced in the InP spectral densities. A slight hardening of the acoustic modes is observed in both materials. Again, the differences between the effective harmonic frequencies associated with the larger amplitude high temperature motions and the small amplitude low temperature motions are due to anharmonicities in the system. Care should be taken in interpreting the absolute width of the spectral density due to the intrinsic uncertainties in the model,

although relative widths and trends across homologous materials are expected to be valid.

## B. (110) Surface Dynamics

The primitive surface unit cell of the zincblende-structure (110) surface contains two atoms, each with three degrees of freedom. (See Fig. 2) Consequently, the six  $q'=0$  modes of the primitive surface unit cell contain two acoustic and four optical modes. As discussed in Section II, the use of a restricted dynamical model causes the acoustic modes to have non-zero energies at  $q'=0$ . For the purposes of this study however, we will focus on the four optical modes.

The computed spectral densities for the GaAs and InP (110) surfaces are shown in Fig. 4, and the surface atomic vibrational energies of the four surface optical modes are summarized in Table III, along with the He-scattering data<sup>15,17,18</sup> and the results of other model computations<sup>18,20</sup> for comparison. It is clear from Table III that the TBMD simulations yield surface vibrational energies that are in quantitative agreement with the available experimental data as well as with the results of other model computations. It is interesting to note that the vibrational energies resulting from a harmonic mode analysis of the GaAs(110)<sup>20</sup> surface differ slightly from those obtained from the TBMD analysis, and that this difference is on the order of the uncertainty induced by the use of a single "special" k-point in the evaluation of the band-structure energy. In fact, this difference results from the use

of different unit cells in the two analyses and thus slightly different integrations performed in the evaluation of the band structure energy and the atomic forces. Given this difference, it follows then that there is no discernable effect of anharmonicity on the energetics of these surface modes. Support for this conclusion comes from the sharpness of the peaks in the computed (110) surface spectral densities (Fig. 4) relative to the peaks in the bulk spectral densities (Fig. 3), for which the anharmonic contributions are significant.

### C. III-V(110)-p(1x1)-Sb Interface Dynamics

The primitive surface unit cell of the Sb-overlayer also contains two atoms and four optical modes. The Raman scattering studies of Hünemann *et al.*<sup>19</sup> identified four optical modes associated with the Sb-overlayer, along with four optical modes they associated with the Sb/InP(110) interface. In this work we will examine the optical modes associated with the Sb-overlayer only. Extension of the restricted dynamical model to encompass vibrations in the top two layers will allow for the examination of the interface modes and these computations are currently underway. Preliminary results indicate that there is only a small shift in the computed overlayer-vibrational energies when the top two layers of the slab are allowed to vibrate versus the case when only the overlayer atoms are allowed to move, providing *a posteriori* support for the use of the restricted dynamical model.

The spectral densities computed for the III-V(110)-p(1x1)-Sb(1ML) interfaces are displayed in Fig. 5. Table IV contains a summary of these results along with the

results of the TBTE normal mode analysis for Sb/GaAs(110)<sup>20</sup> and the Raman scattering data for Sb/InP(110)<sup>19</sup>. As discussed in Section II, the empirical nature of the TBTE parameterization for Sb overlayers makes these results much less certain than those for the clean surfaces. Nevertheless, the qualitative agreement between the TBMD results and the Raman scattering data demonstrated in Table IV is encouraging. Again, the slight differences in the TBTE normal mode analysis and the TBMD results arises from the slightly different integration schemes used, and indicate that, for these modes, there are no significant anharmonicities in the surface potential energy function.

#### IV. Synopsis

Tight-binding molecular dynamics simulations were used to compute the vibrational spectral densities for bulk GaAs and InP, the GaAs(110) and InP(110) surfaces, and the GaAs(110)-p(1x1)-Sb and InP(110)-p(1x1)-Sb interfaces. The results are in quantitative agreement with He-scattering data<sup>15,17,18</sup> for the GaAs(110) surface and in qualitative agreement with scattering data for bulk GaAs and InP and Raman scattering data for the InP(110)-p(1x1)-Sb(1ML) interface<sup>19</sup>. Moreover, the dynamical treatment of these systems allows for the investigation of anharmonic contributions to the vibrational energies through the temperature dependence of the vibrational spectral density. While anharmonic effects were significant in the bulk dynamics, the vibrational energetics of the (110) surface and Sb-interfaces were found to be predominantly harmonic. Finally, these studies demonstrate the utility of quantum-

mechanical molecular dynamics simulations in the investigation of the surface and interfacial atomistic dynamics of semiconductor systems.

Future extensions of this work will focus on the direct determination of the dynamical matrix through generalizations of the velocity autocorrelation function as given by Eqn. 2. In the present study this function corresponds to the trace of the dynamical matrix. Once the dynamical matrix is found, through diagonalization, high temperature generalizations of the eigenmodes are obtained which represent an effective harmonic approximation of the full anharmonic system.

Table I. Parameters used in simulations

	<u>Material</u>	<u>T (K)</u>	<u><math>\Delta t</math> (fsec)</u>	<u># correlations</u>	<u># trials</u>
Bulk	GaAs	300	4.0	4000	90
		77	4.0	4000	30
Surface	GaAs (110)	77	4.0	4000	10
Interface	GaAs (110)-	77	4.0	4000	30
	Sb-(p1x1)-(1ML)				
Bulk	InP	300	2.0	4000	20
		77	2.0	4000	20
		2	2.0	4000	20
Surface	InP (110)	77	4.0	4000	10
Interface	InP (110)-	77	4.0	4000	20
	Sb-(p1x1)-(1ML)				



Table II.

Comparison of TBMD bulk phonon frequencies with experimental and other theoretical results

<u>Material</u>		<u><math>\hbar\omega</math> (meV)</u>			
		TBMD (300K)	Experiment (296K)	Other theory (0K)	
			Ref. 28	Ref.27	Ref. 29
GaAs	$\Gamma$	27.4-28.6	33.2-34.8	37.1	38.1
	X	7.0	9.8		13.1
	X	19.7-20.9	27.1		
	X	23.0-24.2	28.7-31.4		
	"L"	5.4	8.2		
InP	$\Gamma$	29.5-33.5	37.4-43.0		
	X	6.5	8.3		
	X	16.5	23.8		
	X	31-32.5	39.7-41.0		
	"L"	3.8	7.1		

Table III.

Comparison of TBMD (110) surface phonon frequencies with experimental and other theoretical results

<u>Material</u>	TBMD (77K)	<u><math>\hbar\omega</math> (meV)</u>			
		Experiment (296K)		Other theory (0K)	
		Ref.15	Ref. 17	Ref. 18	Ref. 20
GaAs	9.4	10.0	10.0	8.9-10.3	9.3
	16.8				16.4
	23.1				22.0
	24.1				22.9
InP	9.5				
	22.8				
	26.7				
	28.1				

Table IV.

Comparison of TBMD (110)-p(1x1)-Sb interface phonon frequencies with  
experimental and other theoretical results

<u>Material</u>	<u><math>\hbar\omega</math> (meV)</u>		
	TBMD (77K)	Experiment (296K) Ref. 19	other theory (0K) Ref. 20
GaAs	9.7		10.0
	13.6		11.8
	17.2		16.8
	18.5		18.9
InP	9.1	11.9	
	13.2	19.5	
	16.5	20.0	
	17.8	23.0	

### Figure Captions

Figure 1. Cubic 8-atom non-primitive unit cell used in simulations

Figure 2. 15 atomic-layer slab used to model the semi-infinite surface

Figure 3a. GaAs Bulk Spectral Density

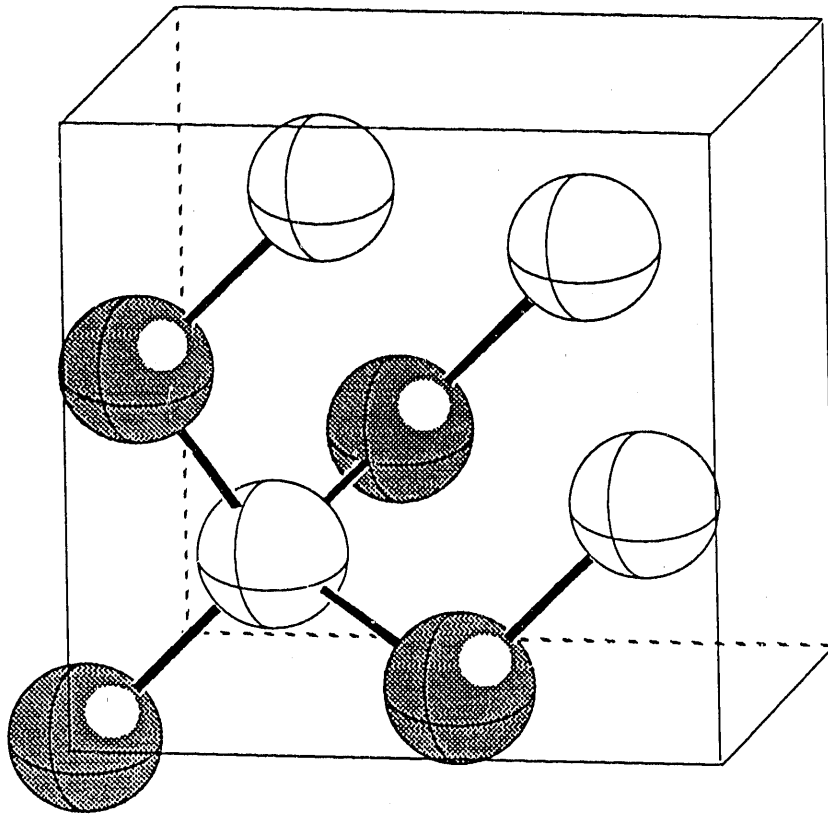
Figure 3b. InP Bulk Spectral Density

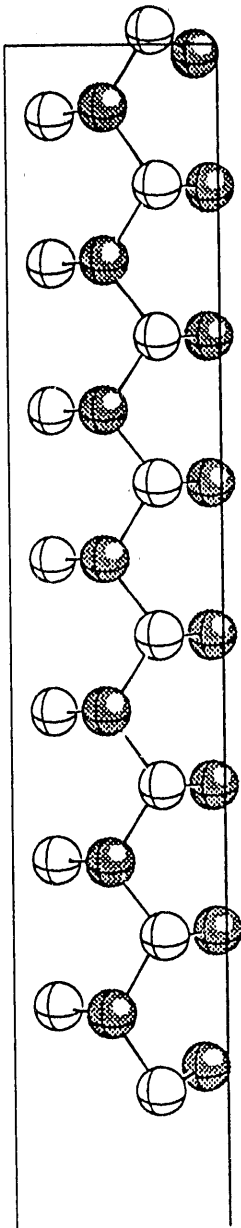
Figure 4a. GaAs (110) Surface Spectral Density, 77K

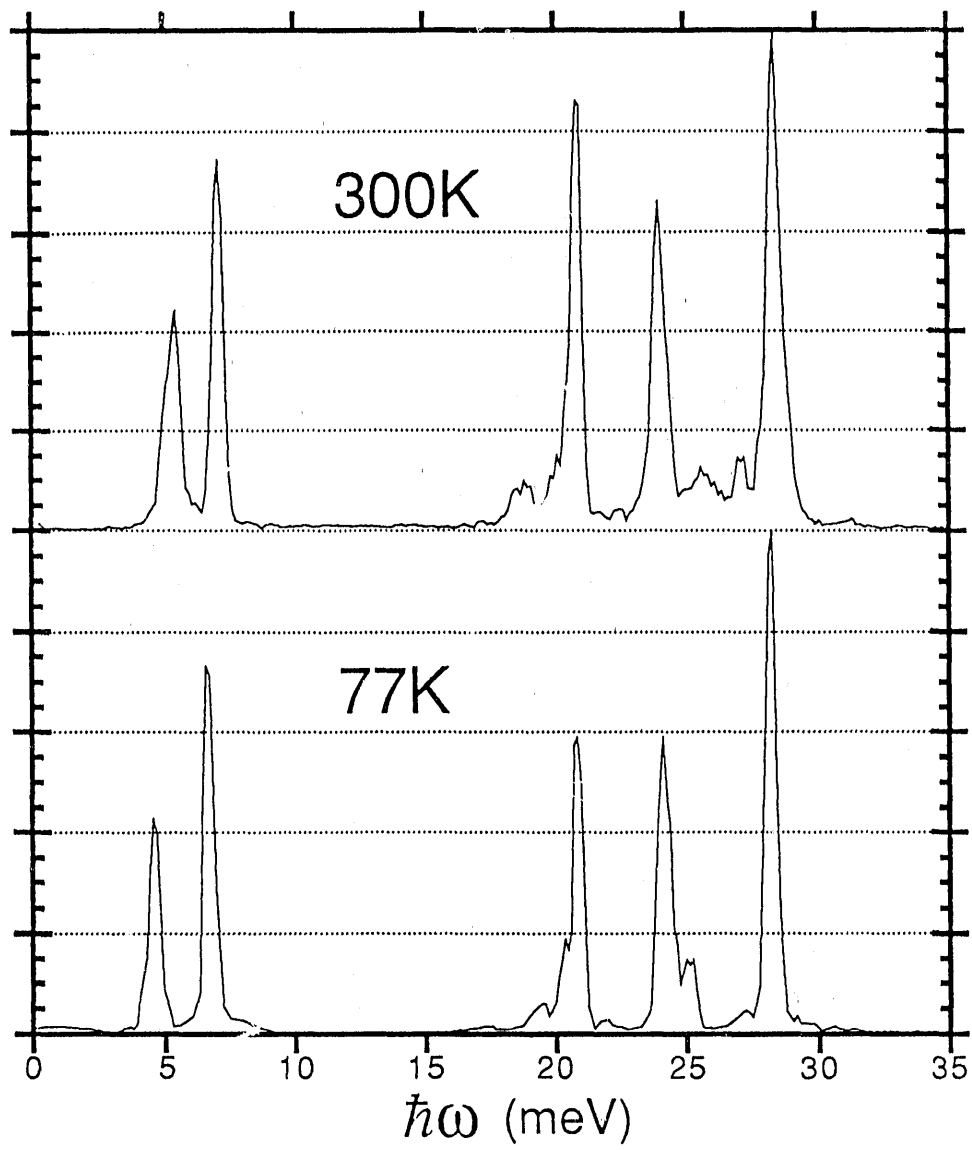
Figure 4b. InP (110) Surface Spectral Density, 77K

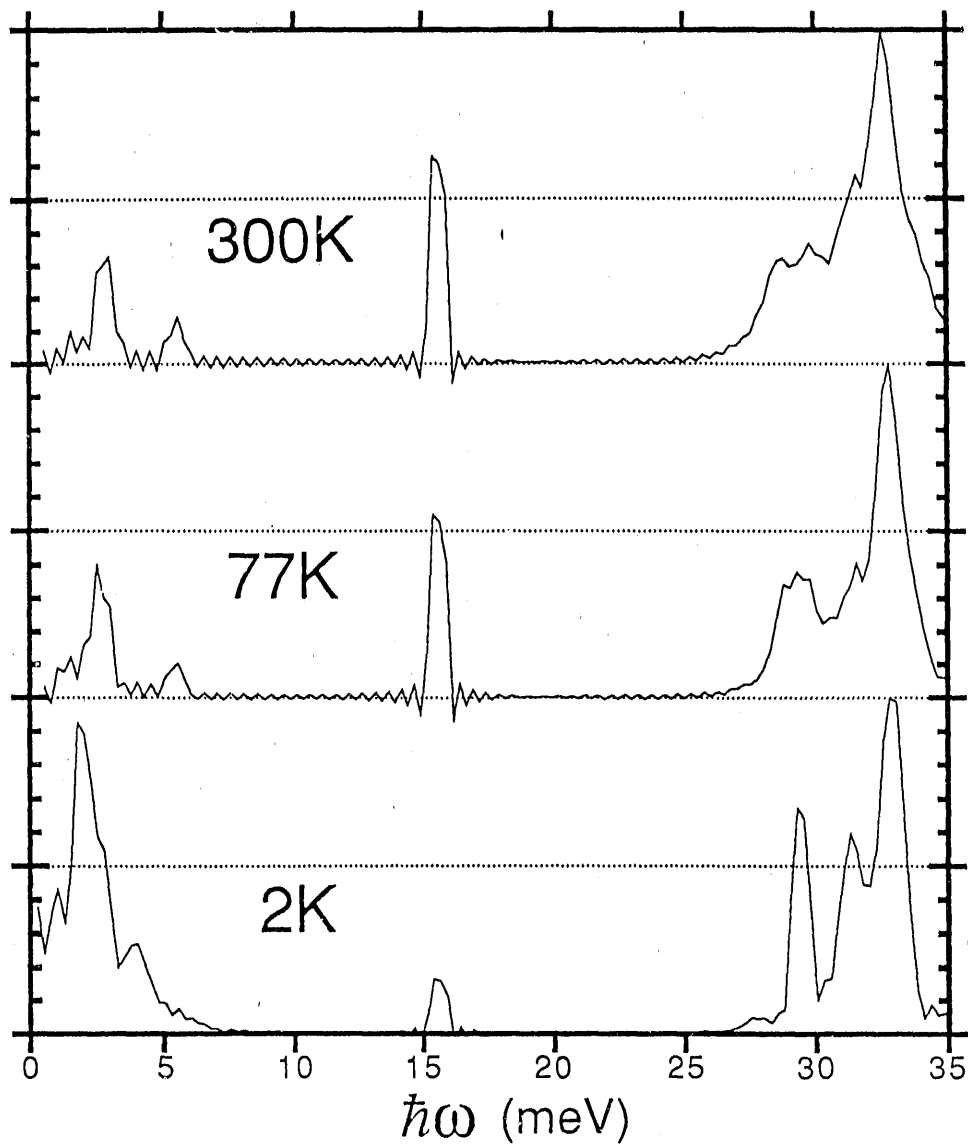
Figure 5a. GaAs (110)-Sb-(p1x1)-(1ML) Spectral Density, 77K

Figure 5b. InP (110)-Sb-(p1x1)-(1ML) Spectral Density, 77K

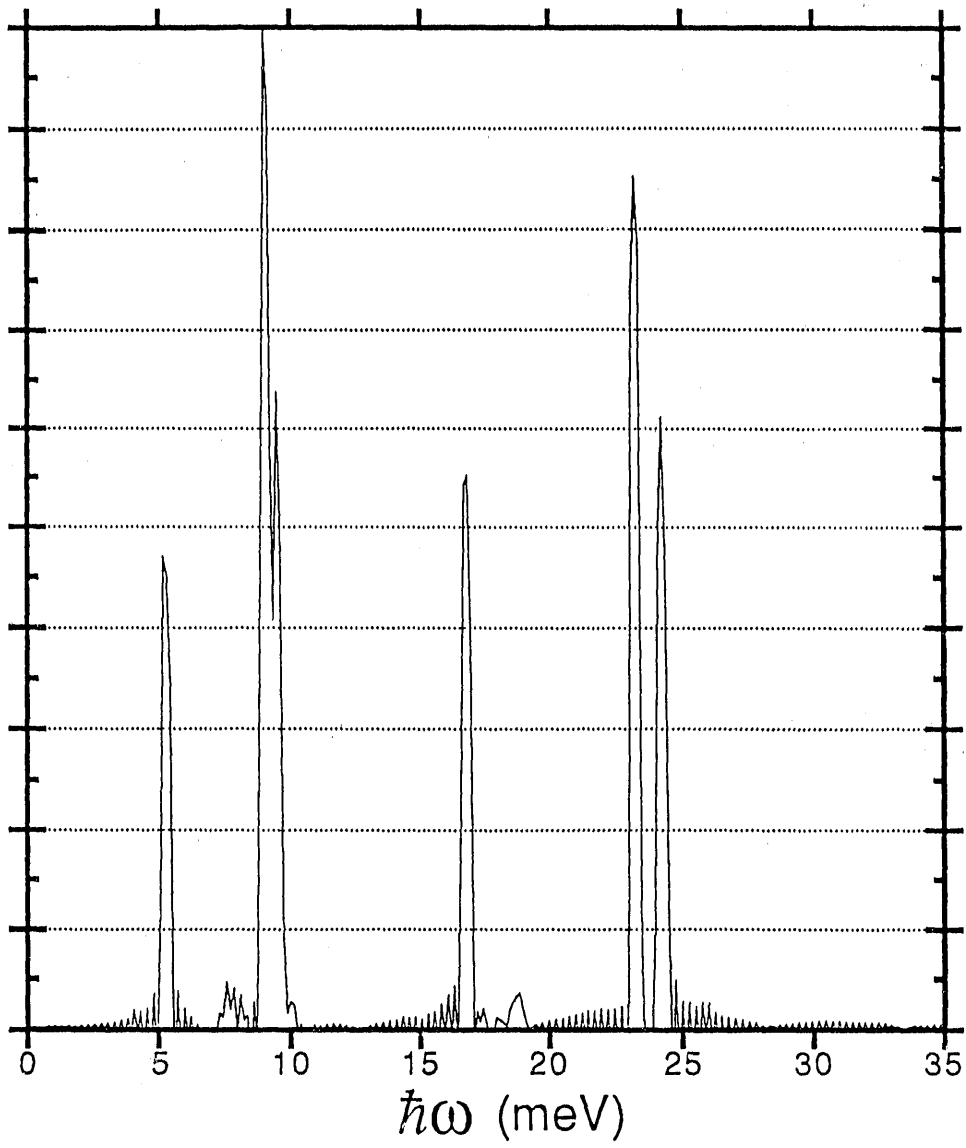


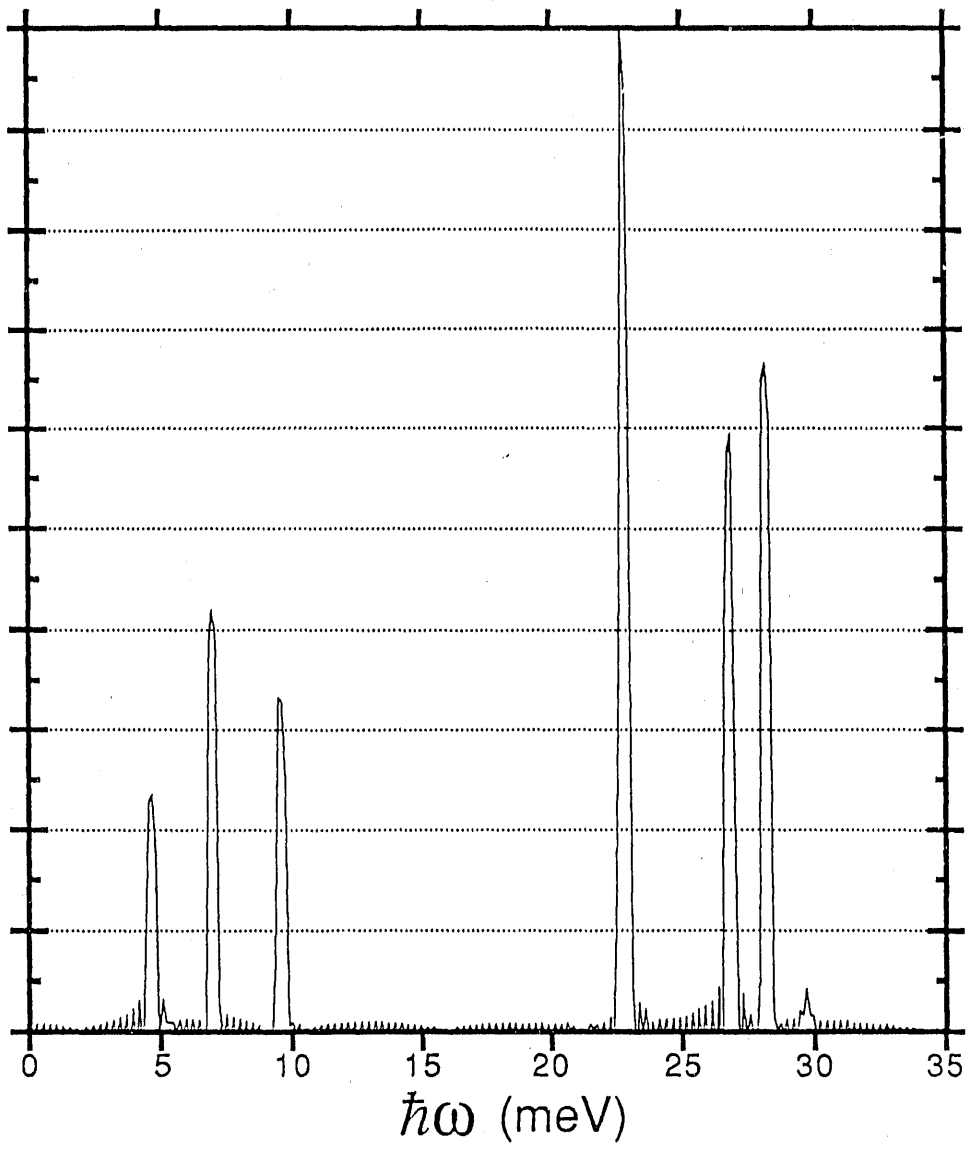


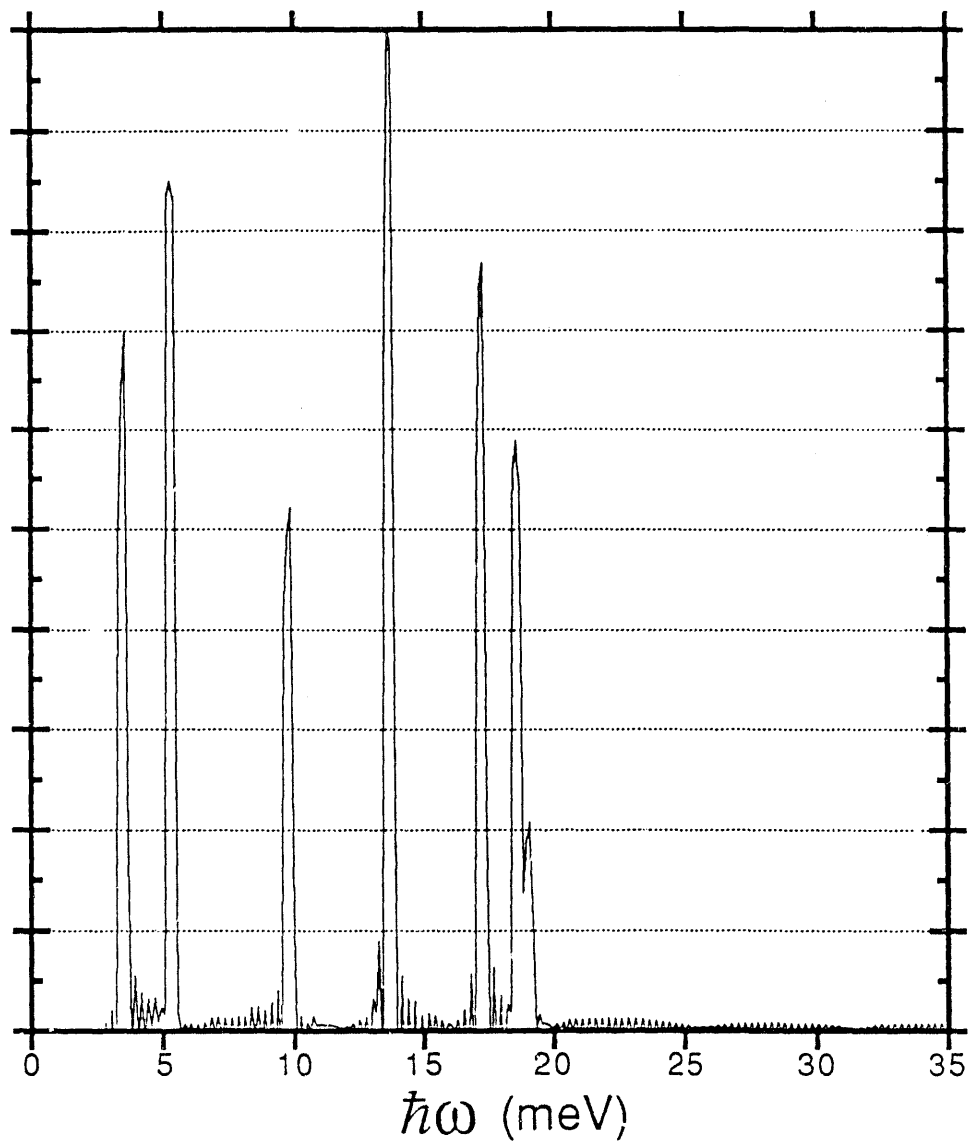


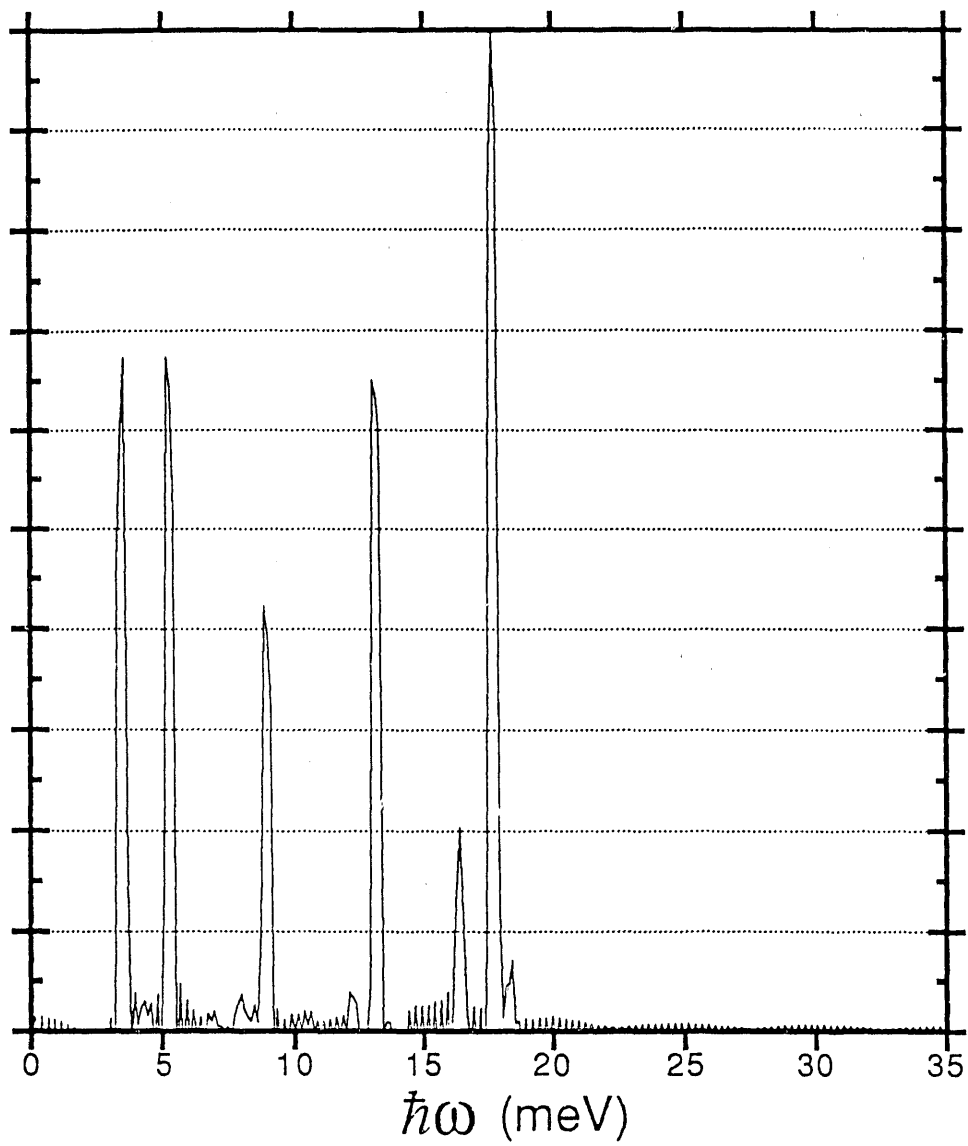












## References

1. R. Car. and M. Parrinello, Phys. Rev. Lett. 55,2471 (1985); 60,204 (1988).
2. (a) O.F. Sankey and D.J. Niklewski, Phys. Rev. B 40,3979 (1989); (b) O.F. Sankey, D.J. Niklewski, D.A. Drabold, and J.D. Dow, Phys. Rev. B 41,12750 (1990); (c) D. A. Drabold, J.D. Dow, S. Klemm, and O.F. Sankey, in *Atomic Scale Calculations of Structure in Materials*, M.A. Schluter and M.S. Daw, Eds., in press.
3. C.Z. Wang, C.T. Chan, and K.M. Ho, Phys. Rev. B 39,8586 (1989).
4. C.Z. Wang, C.T. Chan, and K.M. Ho, Phys. Rev. B 42,11276 (1990).
5. K. Laasonen and R.M. Nieminen, in *Many-Atom Interactions in Solids*, Springer Proceedings in Physics 48, R.M. Nieminen, M.J. Puska, and M.J. Manninen Eds., (Springer-Verlag, Berlin, 1990), p264.
6. F.S. Kahn and J.Q. Broughton, Phys. Rev. B 39, 3688 (1989).
7. M. Menon and R.E. Allen, J. Vac. Sci. Tech. B8,900 (1990); *ibid* B7,729 (1989) and references therein.
8. C.B. Duke, A. Paton, W.K. Ford, A. Kahn, and J. Carelli, Phys. Rev. B 26,803 (1982).
9. W.K. Ford, T. Guo, D.L. Lessor, and C.B. Duke, Phys. Rev. B 42,8952 (1990).
10. T. Kendelewicz, J.C. Woicik, K.E. Miyano, P.L. Cowan, B.A. Karlin, C.E. Bouldin, P. Pianetta, and W.E. Spicer, J. Vac. Sci. Tech. B9,2290 (1991).
11. C. Mailhiot, C.B. Duke, and D.J. Chadi, Phys. Rev. Lett 23,2114 (1984); J. Vac. Sci. Tech. A 3,915 (1985); Surf. Sci. 149,366 (1985).
12. C. Mailhiot, C.B. Duke, and D.J. Chadi, Phys. Rev. B 31,2213 (1985).
13. J.P. LaFemina, C.B. Duke, and C. Mailhiot, J. Vac. Sci. Tech. B8,888 (1990); in *Atomic Scale Calculations of Structure in Materials*, M.A. Schluter and M.S. Daw, Eds., in press.
14. C.B. Duke, J. Vac. Sci. Tech. A6,1957 (1988).
15. U. Harten and J.P. Toennies, Europhys. Lett. 4,833 (1987).
16. Y.R. Wang and C.B. Duke, Surf. Sci. 205,L755 (1988).

17. R.B. Doak and D.B. Nguyen, *J. Elect. Spec. Rel. Phenom.* **44**,205 (1987).
18. P. Santini, L. Miglio, G. Benedek, U. Harten, P. Ruggerone, and J.P. Toennies, *Phys. Rev. B* **42**, 11 942 (1990).
19. M. Hünermann, J. Geurts, and W. Richter, *Phys. Rev. Lett.* **66**,640 (1991).
20. T.J. Godin, J.P. LaFemina, and C.B. Duke, *J. Vac. Sci. Tech.* **B9**,2282 (1991).
21. P. Vogl, H.P. Hjalmarson, and J.D. Dow, *J. Phys. Chem. Solids* **44**,365 (1983).
22. D.J. Chadi, *Phys. Rev. Lett.* **41**,1062 (1978); *Phys. Rev. B* **19**,2074 (1979); *Vacuum* **33**,613 (1983); *Phys. Rev. B* **29**,785 (1984).
23. J.C. Slater and G.F. Koster, *Phys. Rev.* **94**, 1498 (1954).
24. D.J. Chadi and M. Cohen, *Phys. Rev. B* **8**, 5747 (1973).
25. L. Verlet, *Phys. Rev.* **159**, 98 (1967).
26. M.P. Allen and D.J. Tildesley, *Computer Simulation of Liquids* ,(Clarendon, Oxford, 1989).
27. J.A. Majewski, *Acta Physica Polonica* **A75**, 193 (1989).
28. H. Bilz and W. Kress, "Phonon Dispersion Relations in Insulators, Springer Series in Solids State Sciences, Vol 10 (Springer-Verlag, Berlin, 1975) p.105.
29. B.C. Chan and C.K. Ong, *J. Phys. Chem. Solids* **51**,343 (1990).

**END**

**DATE  
FILMED**

*2 / 27 / 92*

